

Impurities block the α to ω martensitic transformation in titanium

RICHARD G. HENNIG^{1*}, DALLAS R. TRINKLE¹, JOHANN BOUCHET², SRIVILLIPUTHUR G. SRINIVASAN², ROBERT C. ALBERS² AND JOHN W. WILKINS¹

¹Department of Physics, Ohio State University, Columbus, Ohio 43210, USA

²Los Alamos National Laboratory, Los Alamos, New Mexico 87545, USA

*e-mail: rhennig@mps.ohio-state.edu

Published online: 23 January 2005; doi:10.1038/nmat1292

Impurities control phase stability and phase transformations in natural and man-made materials, from shape-memory alloys¹ to steel² to planetary cores³. Experiments and empirical databases are still central to tuning the impurity effects. What is missing is a broad theoretical underpinning. Consider, for example, the titanium martensitic transformations: diffusionless structural transformations proceeding near the speed of sound². Pure titanium transforms from ductile α to brittle ω at 9 GPa, creating serious technological problems for β -stabilized titanium alloys. Impurities in the titanium alloys A-70 and Ti-6Al-4V (wt%) suppress the transformation up to at least 35 GPa, increasing their technological utility as lightweight materials in aerospace applications. These and other empirical discoveries in technological materials call for broad theoretical understanding. Impurities pose two theoretical challenges: the effect on the relative

phase stability, and the energy barrier of the transformation. *Ab initio* methods^{4,5} calculate both changes due to impurities. We show that interstitial oxygen, nitrogen and carbon retard the transformation whereas substitutional aluminium and vanadium influence the transformation by changing the d -electron concentration⁶. The resulting microscopic picture explains the suppression of the transformation in commercial A-70 and Ti-6Al-4V alloys. In general, the effect of impurities on relative energies and energy barriers is central to understanding structural phase transformations.

Figure 1a shows the stability range of the titanium phases. The range from 2 to 9 GPa in the published transition pressures of nominally pure titanium^{7,8} is believed to be caused by differences in sample purity^{9–12}. In hydrostatic compression the transformation is suppressed by 1 at% oxygen for short holding times (3–5 min); for

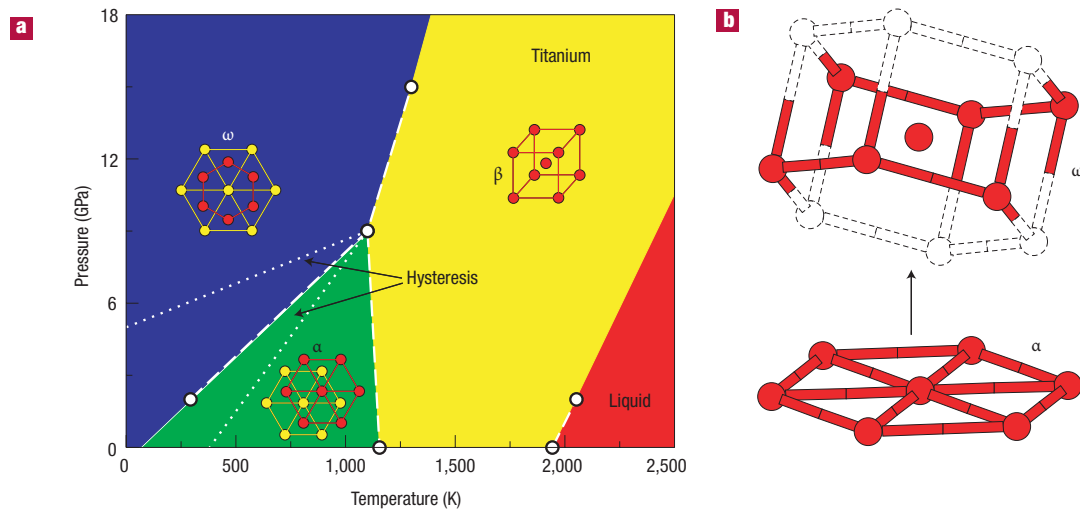


Figure 1 Structural phase transitions in titanium. **a**, The phase diagram of titanium as a function of temperature and pressure shows martensitic transformations between the α , β and ω phases. **b**, The transformation from α to ω proceeds through the TAO-1 mechanism¹³; shown is the transformation of one hexagonal basal plane of α to make the honeycomb and hexagonal planes in ω .

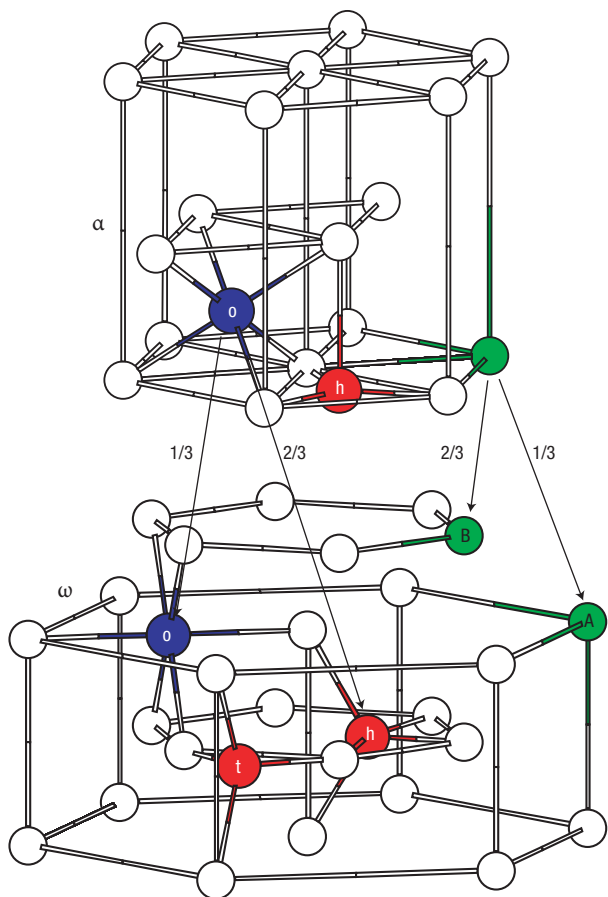


Figure 2 Impurity sites in α and ω . Octahedral (o), tetrahedral (t), and hexahedral (h) sites for interstitial impurities as well as A and B sites for substitutional impurities in the α and ω phases. The α and ω phases each contain one unique o, t and h site. The t site in α relaxes to the nearby h site for all three impurities (O, N, C) and is therefore not shown. The hexahedral site is a distorted double-tetrahedral site with five neighbours. The arrows indicate the transformation of the impurity and lattice sites in the TAO-1 mechanism¹³ and the relative ratios. For clarity, the relative orientation of α and ω in TAO-1 is not shown.

Table 1 Energies and locations of impurities

Site	Wyckoff positions	R_{NN}	Z	E_i (eV)		
				O	N	C
a Interstitial impurities						
α_{oct}	2(a)	(0, 0, 0)	2.06–2.09	6	-6.12	-5.10
α_{hex}	2(d)	(2/3, 1/3, 1/4)	1.91–1.95	5	-4.93	-3.41
ω_{oct}	3(f)	(1/2, 0, 0)	2.03–2.17	6	-6.06	-4.99
ω_{hex}	6(m)	(x, 2x, 1/2)	1.92–2.18	5	-4.47	-3.03
ω_{tet}	6(k)	(x, 0, 1/2)	1.90–2.02	4	-4.38	-2.83
b Substitutional impurities						
				Al		V
α	2(c)	(1/3, 2/3, 1/4)	2.85–2.92	12	-0.88	+0.51
ω_A	1(a)	(0, 0, 0)	2.82–3.00	14	-0.90	+0.60
ω_B	2(d)	(1/3, 2/3, 1/2)	2.60–3.00	11	-0.47	+0.33

The formation energies and locations of interstitial and substitutional impurities in the α ($P6_3/mmc$) and ω ($P6/mmm$) phases are given. The formation energies E_i for O, N, and C are measured relative to molecular O_2 , N_2 and graphite, respectively, and for Al and V relative to their f.c.c. and b.c.c. phases, respectively. All calculations are done at 1 at% defect concentration. Comparing the formation energies with the calculations for 2 at% impurity concentration estimates a finite size error of 0.05 eV. The Wyckoff multiplicities, labels and positions¹⁶ of the impurity sites are listed. For each site, the nearest-neighbour distances after relaxation, R_{NN} , are similar for all impurity species; hence, we show the range of values. For comparison, R_{NN} is 2.89 Å in α and 2.84–3.01 Å for ω_A and 2.65–3.01 Å for ω_B . The coordination number Z at each site is also listed.

long holding times (10 min) there is a diffusion-controlled recurrence of the transformation⁹. In shock experiments¹⁰ two commercial titanium alloys, A-70 and Ti-6Al-4V, show no transformation up to 35 GPa.

Our approach exploits the basic observation that for any martensitic transformation the speed of the transformation traps impurities in their local environment. Using the recently discovered $\alpha \rightarrow \omega$ transformation pathway¹³, we study interstitial O, N and C, and substitutional Al and V. Figure 1b illustrates the TAO-1 mechanism¹³, whose energy barrier of 9 meV atom⁻¹ is at least four times lower than any other pathway and remains lowest even when nucleation effects are considered¹³. Molecular dynamics simulations for the $\alpha \rightarrow \omega$ transformation in pure titanium show that the TAO-1 mechanism provides a mobile interface¹⁴.

Figure 2 shows the location of interstitial impurities and the effect of the transformation on these sites. The interstitial impurity sites were found by placing O, N, and C impurities on all interstitial sites in α and ω and relaxing the atomic positions. Each phase contains one unique octahedral, tetrahedral and hexahedral site. However, the tetrahedral site in α is unstable for O, N and C and relaxes to the nearby hexahedral site in the basal plane. The ‘hexahedral’ site is a distorted double-tetrahedral site with five neighbours, formed by a triangle of the basal plane and the two atoms right above and below the centre of the triangle. The instability of the tetrahedral site is unexpected from crystallographic considerations¹⁵ and is due to atomic relaxations. In ω the tetrahedral and hexahedral sites are both stable, and they are close in energy and location.

Table 1a shows the formation energies of the interstitial defects in α and ω . The energies of O, N and C are measured relative to molecular O_2 , N_2 and graphite, respectively. For both α and ω the

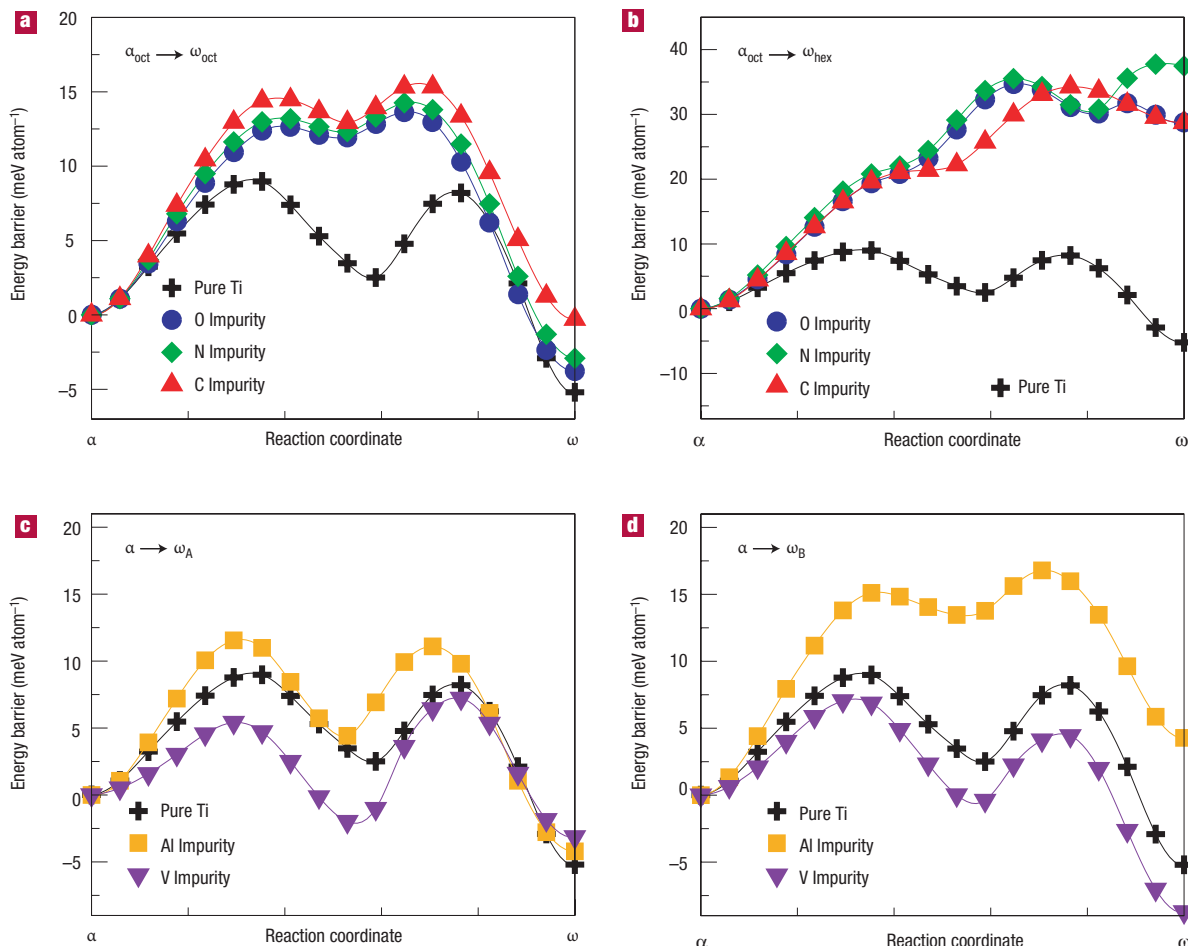


Figure 3 Impurities change the energy barrier of the $\alpha \rightarrow \omega$ transformation. The energy barriers for the TAO-1 transformation of interstitial and substitutional impurities in titanium are shown relative to the α phase in units of meV atom⁻¹. The defect concentration is 2 at%. The endpoint energies match the formation energies of Table 1 for a defect concentration of 1 at% within 1 meV atom⁻¹, providing an accuracy estimate for the barrier. The interstitial O, N and C impurities occupy the α_{oct} and transform into either **a**, ω_{oct} or **b**, ω_{hex} , with a 1:2 ratio. The substitutional Al and V impurities transform in ω to either **c**, the A site or **d**, the B site, with a 1:2 ratio.

octahedral site is more stable than the tetrahedral or hexahedral sites. This is simply related to the size of the interstitial sites: larger sites have lower formation energies. Comparison between the α and ω interstitial impurities shows that the octahedral formation energy is slightly lower for α ; this difference shifts the relative energy of the two crystal structures, decreasing the stability of ω relative to α .

Figures 3a and b show that octahedral sites in α (favoured by O, N and C) transform into two possible sites in ω and increase the energy barrier for the transformation. The TAO-1 pathway breaks the hexagonal symmetry and transforms a third of the octahedral sites into the ω octahedral site and two-thirds into the ω hexahedral site. The presence of impurities increases the energy barrier regardless of the final site of the impurities; however, this increase is much larger for the octahedral to hexahedral pathway than for octahedral to octahedral. For all three impurities, despite their different chemistry, their similar size results in nearly identical barriers.

Table 1b shows the formation energies of the substitutional Al and V in α and the A and B sites of ω . These energies are defined relative to f.c.c. Al and b.c.c. V. Comparison between the α and ω substitutional impurities shows that, for both Al and V, the favoured ω site is lower than the α site. During the transformation, however,

a random mixture of ω occupations will be produced in a 1:2 ratio as shown in Fig. 2. In that case, the formation energy combination $\omega_A/3 + 2\omega_B/3$ is lower than α for V, and higher for Al. This is expected to increase the stability of ω relative to α for V and decrease it for Al.

Figure 3c and d show how the α substitutional sites for Al and V transform to the two possible ω sites and affect the transformation barrier. The TAO-1 pathway lowers the symmetry and transforms a third of the α sites into ω_A sites and two-thirds into ω_B sites. The presence of impurities changes the energy barrier in a fashion similar to the formation energies. The shift in the barrier matches the shift in the relative energies of α and ω ; both are consistent with the change in d -electron concentration⁶. The d -electron effect is also observed in the alloying behaviour⁶: transition metals with more d electrons such as V, Mo, Fe and Ta stabilize the ω phase, whereas early transition metals and simple metals such as Al favour α .

The $\alpha \rightarrow \omega$ phase transition is sensitive to small energy changes. At zero pressure and temperature, the ω phase is about 4 meV atom⁻¹ lower in energy than α (ref. 17) and the energy barrier from α to ω is 9 meV atom⁻¹ (ref. 13). It takes 9 GPa to overcome the energy barrier in shock experiments¹⁰ or 280 K to overcome the energy difference¹⁸. Hence, we expect a marked change in transition temperature and pressure owing to the energy shift caused by impurities.

Table 2 shows the effect of impurities in A-70 and Ti-6Al-4V, especially the effect of O and Al. Overall, we find that the presence of impurities in both alloys suppresses the $\alpha \rightarrow \omega$ transformation by increasing both the ω energy relative to α , and the energy barrier. The energy barrier increase is too small to make any other pathway energetically more favourable¹³, but it is expected to reduce nucleation, slow down the transformation and increase the pressure hysteresis. The change of the α - ω energy difference shifts the α - ω phase boundary¹⁸ upwards in pressure by several gigapascals and thus at room temperature greatly increases the stability range of ω .

The other interstitial impurities, N and C, have an effect similar to O. Despite their different chemistry, all increase the energy barrier and the relative energy by nearly the same amount. This indicates the primary effect is steric, and hence we expect other interstitials of comparable size to have similar effects. In the A-70 and Ti-6Al-4V alloys the effect of N and C is smaller in proportion to their lower concentration.

In contrast, the substitutional Al and V impurities have opposite effects due to the change in d -electron concentration. As expected from the alloying behaviour of titanium^{6,11}, V decreases the energy of ω and Al increases it. We observe the same behaviour for the energy barriers. The Al impurity reduces the d -electron number by two, whereas V increases it by one; thus Al has a larger effect on the $\alpha \rightarrow \omega$ transformation. The commercial Ti-6Al-4V alloy contains both; however, the concentration of Al (11 at%) is three times higher than the concentration of V (4 at%).

A simple estimate of the transition pressure uses the shift of the α - ω energy difference and the increase of the energy barrier. The equilibrium transition pressure is where the enthalpies are equal: -3 GPa for pure titanium, 6 GPa for A-70 and 13 GPa for Ti-6Al-4V. The hysteresis pressure p_h follows from the energy barrier¹⁹: $E_b = p_h \Delta V / 2$. Using $\Delta V = 0.3 \text{ \AA}^3$ yields the hysteresis pressures: 11 GPa for pure titanium, 25 GPa for A-70 Ti, and 50 GPa for Ti-6Al-4V. Summing the equilibrium transition pressure and the hysteresis pressure estimates the transition pressure. For pure titanium the estimate of 8 GPa matches the observed value. For A-70 and Ti-6Al-4V the estimates of 31 GPa and 63 GPa explain the observed suppression of the martensitic $\alpha \rightarrow \omega$ transformation in hydrostatic and shock experiments.

At room temperature, entropic contributions to the free energy are not expected to alter the effect of impurities on the energy differences and barriers. For pure titanium the entropy difference between α and ω is $0.1 k_B \text{ atom}^{-1}$ corresponding to an energy change at room temperature of 3 meV atom^{-1} (ref. 18). Impurity concentrations of less than 10 at% will probably change the entropy difference by much less than the 3 meV atom^{-1} for pure titanium. Hence, the free energy change due to the impurities is dominated by the energy.

We conclude that by determining the energy and location of impurities in α and ω titanium it is possible to show how they suppress the martensitic $\alpha \rightarrow \omega$ transformation. Our approach makes use of the basic observation that for any martensitic transformation the impurities are trapped in their local environment. The effect of impurities on relative energies and energy barriers is central to understanding structural phase transformations.

METHODS

The *ab initio* calculations are performed with VASP^{4,20}, a density functional code using a plane-wave basis and ultrasoft Vanderbilt type pseudopotentials^{21,22}. The generalized gradient approximation of Perdew and Wang is used²³. A plane-wave kinetic-energy cutoff of 400 eV ensures energy convergence to $0.3 \text{ meV atom}^{-1}$. The k -point meshes for the different structures are chosen to guarantee an accuracy of 1 meV atom^{-1} . For titanium we treat the $3p$ states as valence states in addition to the usual $4s$ and $3d$ states to give an accurate treatment of the interaction at close interatomic distances. For the other elements the pseudopotentials describe the core states as follows: V [Ar], Al [Ne], O, N and C [He].

Impurity locations and formation energies are determined by relaxations for a single impurity atom in a 96-atom ($4 \times 4 \times 3$) supercell for α and a 108-atom ($3 \times 3 \times 4$) supercell for ω with a $2 \times 2 \times 2$ k -point sampling grid. This results in a 1 at% impurity concentration. The atom positions are relaxed until the atomic-level forces are smaller than 20 meV \AA^{-1} .

Nudged elastic band calculations⁵ with variable cell shape at constant pressure yield the energy barriers of the martensitic transformation. The pathway is represented by 16 intermediate images of a 48-Ti-atom supercell with one impurity constructed using $2\sqrt{2} \times \sqrt{2} \times 2$ cells of the TAO-1 mechanism with a $4 \times 4 \times 4$ k -point mesh. This results in an impurity concentration of 2 at%. The atom positions and the simulation cells are relaxed until the atomic-level forces are smaller than 50 meV \AA^{-1} and the stresses are smaller than 20 MPa. Comparing the energies for the 48-atom supercell with the ones for the larger cells of 96 and 108 atoms and 1 at% impurity concentration provides an estimate of the finite size error for the defect energies of 0.05 eV and for the energy barrier calculation of 1 meV atom^{-1} . Combining the finite size error with the k -point mesh and cutoff energy accuracy yields an energy barrier accuracy of 2 meV atom^{-1} .

Received 29 January 2004; accepted 13 October 2004; published 23 January 2005.

References

- Otsuka, K. & Wayman, C. M. (eds) *Shape Memory Materials* (Cambridge Univ. Press, 1998).
- Olson, G. B. & Owen, W. S. (eds) *Martensite* (ASM, Metals Park, Ohio, 1992).
- Vocadlo, L. *et al.* Possible thermal and chemical stabilization of body-centred-cubic iron in the Earth's core. *Nature* **424**, 536–539 (2003).
- Kresse, G. & Hafner, J. *Ab initio* molecular dynamics for liquid metals. *Phys. Rev. B* **47**, 558–561 (1993).
- Jónsson, H., Mills, G. & Jacobsen, K. W. In *Classical and Quantum Dynamics in Condensed Phase Simulations* (eds Berne, B. J., Ciccotti, G. & Coker, D. F.) 385–404 (World Scientific, Singapore, 1998).
- Vohra, Y. K. Electronic basis for omega phase stability in group IV transition metals and alloys. *Acta Metall.* **27**, 1671–1674 (1979).
- Jayaraman, A., Klement, J. W. & Kennedy, G. C. Solid-solid transitions in titanium and zirconium at high pressures. *Phys. Rev.* **131**, 644–649 (1963).
- Zilbershtein, V. A. *et al.* Alpha-omega transition in titanium and zirconium during shear deformation under pressure. *Fiz. Met. Metalloved.* **39**, 445–447 (1975).
- Vohra, Y. K., Sikka, S. K., Vaidya, S. N. & Chidambaram, R. Impurity effects and reaction kinetics of the pressure-induced alpha to omega transformation in Ti. *J. Phys. Chem. Solids* **38**, 1293–1296 (1977).
- Gray, G. T., Morris, C. E. & Lawson, A. C. In *Titanium '92: Science and Technology* (eds Froes, F. H. & Caplan, I. L.) 225–232 (TMS, Warrendale, 1993).
- Sikka, S. K., Vohra, Y. K. & Chidambaram, R. Omega phase in materials. *Prog. Mater. Sci.* **27**, 245–310 (1982).
- Greeff, C. W., Trinkle, D. R. & Albers, R. C. Shock-induced α - ω transition in titanium. *J. Appl. Phys.* **90**, 2221–2226 (2001).
- Trinkle, D. R. *et al.* New mechanism for the α to ω martensitic transformation in pure titanium. *Phys. Rev. Lett.* **91**, 025701 (2003).
- Trinkle, D. R. *A Theoretical Study of the Hcp to Omega Martensitic Phase Transition in Titanium* Thesis, Ohio State Univ. (2003).
- Conrad, H. Effect of interstitial solutes on the strength and ductility of titanium. *Prog. Mater. Sci.* **26**,

Table 2 Impurity effects in commercial alloys

Alloy	Impurity	$\Delta E_{\omega-\alpha}$	ΔE_b
A-70	O (1.10 at%)	+12	+10
	N (0.08 at%)	+1	+1
	C (0.07 at%)	+1	+1
	Total	+14	+12
Ti-6Al-4V	Al (10.7 at%)	+29	+31
	V (3.8 at%)	-3	-3
	O (0.5 at%)	+6	+5
	Total	+33	+33

The impurities present in the commercial A-70 and the Ti-6Al-4V alloys change the relative energy between α and ω and the energy barrier of the martensitic transformation. The shifts in the relative energy $\Delta E_{\omega-\alpha}$ and energy barriers ΔE_b are given by Table 1 and Fig. 3, respectively, in units of meV atom^{-1} . Both are scaled to the experimental impurity concentrations given in ref. 10. For small concentrations, the effects of the impurities are additive and linear in the concentration. In pure titanium ω is 4 meV atom^{-1} lower in energy than α and the α - ω energy barrier is 9 meV atom^{-1} .

- 123–404 (1981).
16. Hahn, T. (ed.) *International Tables for Crystallography* Vol. A. (Kluwer, Dordrecht, 1996).
17. Kuteпов, А. Л. & Kuteпova, С. Г. Crystal structures of Ti under high pressure: theory. *Phys. Rev. B* **67**, 132102 (2003).
18. Rudin, S. P., Jones, M. D. & Albers, R. C. Thermal stabilization of the hcp phase in titanium. *Phys. Rev. B* **69**, 094117 (2004).
19. Estrin, E. I. Concerning polymorphous (normal, martensitic) transformations. *Fiz. Met. Metalloved.* **37**, 1249–1255 (1974).
20. Kresse, G. & Furthmüller, J. Efficient iterative schemes for ab initio total-energy calculations using a plane-wave basis set. *Phys. Rev. B* **54**, 11169–11186 (1996).
21. Vanderbilt, D. Soft self-consistent pseudopotentials in a generalized eigenvalue formalism. *Phys. Rev. B* **41**, 7892–7895 (1990).
22. Kresse, G. & Hafner, J. Norm-conserving and ultrasoft pseudopotentials for first-row and transition elements. *J. Phys. Condens. Matter* **6**, 8245–8257 (1994).
23. Perdew, J. P. in *Electronic Structure of Solids '91*. (eds Ziesche, P. & Eschrig, H.) 11–20 (Akademie, Berlin, 1991).

Acknowledgements

This research is supported by DOE Grants No. DE-FG02-99ER45795 (OSU) and No. W-7405-ENG-36 (LANL). Computational resources were provided by the Ohio Supercomputing Center, NERSC, and QSC at LANL. We thank G. T. Gray and M. Asta for helpful discussions. Correspondence and requests for materials should be addressed to R.G.H.

Competing financial interests

The authors declare that they have no competing financial interests.